Inactivation of Two Diverse Enzymes in the Amidinotransferase Superfamily by 2-Chloroacetamidine: Dimethylargininase and Peptidylarginine Deiminase†

Everett M. Stone,‡ Terezie H. Schaller,§ Helena Bianchi,|| Maria D. Person,⊥ and Walter Fast*,‡,§,||

Divisions of Medicinal Chemistry and Pharmacology and Toxicology, College of Pharmacy, and Graduate Programs in Biochemistry and Cell and Molecular Biology, The University of Texas, Austin, Texas 78712

Received July 12, 2005; Revised Manuscript Received August 11, 2005

ABSTRACT: The enzymes dimethylargininase [dimethylarginine dimethylaminohydrolase (DDAH); EC 3.5.3.18] and peptidylarginine deiminase (PAD; EC 3.5.3.15) catalyze hydrolysis of substituted arginines. Due to their role in normal physiology and pathophysiology, both enzymes have been identified as potential drug targets, but few useful inhibitors have been reported. Here, we find that 2-chloroacetamidine irreversibly inhibits both DDAH from *Pseudomonas aeruginosa* and human PAD4 in a time- and concentration-dependent manner, despite the nonoverlapping substrate specificities and low levels of amino acid identity of their catalytic domains. Substrate protection experiments indicate that inactivation occurs by modification at the active site, albeit with modest affinity. Mass spectral analysis demonstrates that irreversible inactivation of DDAH occurs through selective formation of a covalent thioether bond with the active-site Cys249 residue. The mechanism of inactivation by 2-chloroacetamidine is analogous to that of chloromethyl ketones, a set of inhibitors that have found wide application because of their specific covalent modification of active-site residues in serine and cysteine proteases. Likewise, 2-chloroacetamidine may potentially find wide applicability as a general pharmacophore useful in delineating characteristics of the amidinotransferase superfamily.

The amidinotransferase superfamily contains a diverse set of enzymes, including hydrolases, dihydrolases, and amidinotransferases, that all use substrates structurally related to L-arginine (*1, 2*). Although the particular substrates and products of these enzymes differ, their catalytic mechanisms are proposed to proceed through similar covalent *S*-alkylthiouronium intermediates formed by nucleophilic attack of an active-site Cys residue (*1*). Several of the enzymes in this superfamily have been suggested as potential drug targets (*1*−*4*), but in general, there have been few useful inhibitors reported (*5*−*8*). Here, we will focus on the inhibition of two diverse members of this superfamily, dimethylargininase [dimethylarginine dimethylaminohydrolase (DDAH);[1] EC 3.5.3.18] and peptidylarginine deiminase (PAD; EC 3.5.3.15).

In humans, DDAH isoforms regulate concentrations of N^{ω}-methyl-L-arginine (**1**) and N^{ω},N^{ω}-dimethyl-L-arginine that serve as endogenous nitric oxide synthase inhibitors by hydrolyzing these compounds to citrulline (**2**) and their corresponding alkylamine (Scheme 1A) (*3*). Dysregulation of nitric oxide production is implicated in numerous disease states, including septic shock, neuronal damage during stroke, and angiogenesis (*3*), so understanding the normal physiological control mechanisms of nitric oxide production is of significant interest as is the ability to modulate the concentration of endogenous methylated arginines through the

Scheme 1: Hydrolysis Reactions Catalyzed by DDAH (A) and PAD (B)

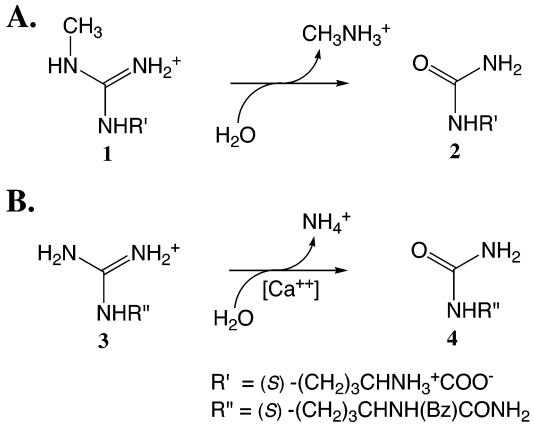

† This research was supported by the American Heart Association (SDG 0435178N), the Robert A. Welch Foundation (F-1572), the Arthritis National Research Foundation, and the American Cancer Society (RSG-05-061-01-GMC). Mass spectra were acquired in the CRED Analytical Core, which is supported by NIEHS Grant ES07784.

* To whom correspondence should be addressed: College of Pharmacy, PHAR-MED CHEM, The University of Texas, 1 University Station, A1935, Austin, TX 78712. Phone: (512) 232-4000. Fax: (512) 232-2606. E-mail: WaltFast@mail.utexas.edu.

‡ Graduate Program in Cell and Molecular Biology.

§ Division of Medicinal Chemistry, College of Pharmacy.

|| Graduate Program in Biochemistry.

⊥ Division of Pharmacology and Toxicology, College of Pharmacy.

[1] Abbreviations: •NO, nitric oxide; DDAH, dimethylarginine dimethylaminohydrolase; PAD, peptidylarginine deiminase; *Pa*, *Pseudomonas aeruginosa*; GST, glutathione transferase; His_6, hexahistidine affinity tag; ATCC, American Type Culture Collection; Bz, benzoyl; ESI-MS, electrospray ionization mass spectrometry; MALDI-TOF, matrix-assisted laser desorption ionization time-of-flight; PSD, post-source decay; Acam, acetamidine; LB, Luria-Bertani; PCR, polymerase chain reaction; SDS−PAGE, sodium dodecyl sulfate−polyacrylamide gel electrophoresis; OD_{600}, optical density at 600 nm; ORF, open reading frame; SAR, structure−activity relationship.

10.1021/bi051341y CCC: $30.25
Published on Web 09/29/2005

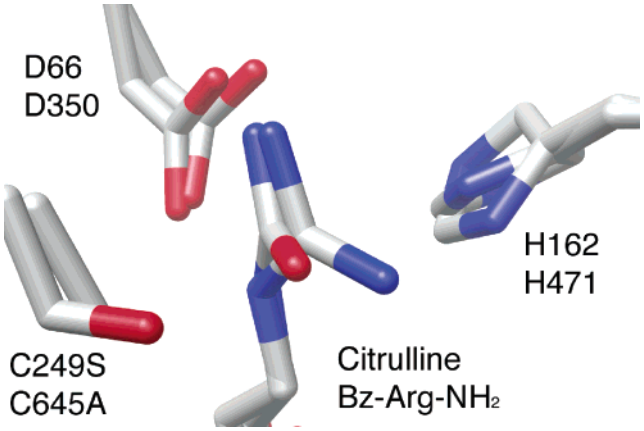

FIGURE 1: Active-site comparison of DDAH and PAD. Superimposed structures of a citrulline-bound C249S mutant *Pa* DDAH (coordinates from PDB entry 1H70) and N^{α}-benzoyl-L-arginine amide-bound C645A mutant PAD4 (PDB entry 1WDA) show close alignment of active-site residues (*11*, *19*). Labels list the residue identification numbers of DDAH above those of PAD.

selective inhibition of DDAH activity. The bacterium *Pseudomonas aeruginosa* (*Pa*) also harbors a DDAH (*9*) that may be related to its pathogenicity; one report suggests that nitric oxide may mediate respiratory tissue damage during infection, an effect limited by N^{ω},N^{ω}-dimethyl-L-arginine (*10*), but possibly enhanced by *Pa* DDAH. Hence, inhibitors for both human and microbial DDAH isoforms are desired. Inhibitors known to target the active site specifically include L-citrulline (*11*, *12*), L-homocysteine (*6*), *S*-nitroso-L-homocysteine (*5*), zinc(II) (*13*), and synthetic arginine analogues (*8*). However, few specific irreversible inhibitors have been described (*5*).

Human PAD isoforms hydrolyze peptidylarginine residues (**3**) to peptidylcitrulline (**4**) and ammonia (Scheme 1B) and, unlike DDAH isoforms, are regulated by calcium (*4*). PAD activity has been linked to disease states, including multiple sclerosis and rheumatoid arthritis, and one human isoform, PAD4, has been under intense study for its reported role in removing methylamine from nuclear receptor coactivators and histones previously methylated by the protein arginine methyltransferases (*4*, *14*−*17*). Although inhibition of PAD activity has also been proposed as a therapeutic goal, less work has been reported describing inhibitory compounds (*7*, *18*). Notably, paclitaxel is a noncompetitive inhibitor of one mammalian PAD (*18*).

The amino acid sequences of the α/β propeller domains of DDAH and PAD are only 18% identical, and as often observed among diverse members of a superfamily, these enzymes do not effectively hydrolyze each other's substrates. However, both of these enzymes do have strong similarities at their active sites, including a cysteine residue that is proposed as the catalytic nucleophile, an aspartate residue that binds two of the three nitrogens in the substrate's guanidinium, and a histidine residue also thought to play a role in catalysis (Figure 1) (*11*, *19*). Because of these strong active-site similarities, it is reasonable to propose that a general inhibitor for this class of enzymes can be developed. On the basis of the observation that the active-site Cys of DDAH forms a covalent adduct during turnover by attacking the substrate (*20*), we reasoned that placing a good leaving group on a substrate-like ligand may result in covalent inactivation. Therefore, 2-chloroacetamidine, having a substrate-like amidinium group and a chloromethylene moiety, seemed to be a likely candidate. This compound is analogous to the chloromethyl ketone inactivators that have found wide application because of their specific covalent modification of active-site residues in serine (*21*) and cysteine (*22*) proteases (*23*, *24*). Here, we report that 2-chloroacetamidine is indeed an irreversible, time- and concentration-dependent, active-site-directed inactivator of both *Pa* DDAH and human PAD4. The mechanism of DDAH inactivation is studied in detail, and the process is found to occur by selective modification of the active-site Cys residue. To our knowledge, this work describes the first inactivator that works on diverse members of the amidinotransferase superfamily.

MATERIALS AND METHODS

Materials. Synthetic DNA primers were from Sigma-Genosys (The Woodlands, TX). Restriction enzymes and dNTPs were from New England Biolabs (Beverly, MA). Triplemaster polymerase was from Eppendorf (Westbury, NY). Qiaquick purification kits were from Qiagen (Valencia, CA). Glu-C endoproteinase was from Roche (Indianapolis, IN). 2-Chloroacetamidine was from Lancaster (Windham, NH). Chelex-100 was from Bio-Rad (Hercules, CA). Unless noted otherwise, all other chemicals and buffers are from Sigma-Aldrich Chemical Co. (St. Louis, MO).

Construction of an Expression Vector for Mutant H162G DDAH, Protein Expression, and Purification. Two complementary mutagenic oligonucleotides, (forward) 5′-CGCCTGGAAAAGGTCCTGggcCTGAAGACCGGGCTCGCC-3′ and (reverse) 5′-GGCGAGCCCGGTCTTCAGgccCAGGACCTTTTCCAGGCG-3′, were designed to introduce a mutant codon (lowercase) encoding a H162G mutation in the DDAH sequence by overlap extension PCR (*25*). Briefly, a 3′ H162G megaprimer was produced by PCR amplification from a pETpaDH template (*20*) using the forward mutagenic primer and an outside T7 terminator primer (New England Biolabs) in an MJ Research (Waltham, MA) PTC 200 thermocycler, along with dNTPs, Triplemaster polymerase, and Hi-Fidelity Buffer (Eppendorf), with a temperature program of 95 °C for 5 min, followed by 30 cycles of 95 °C for 30 s, 52 °C for 30 s, and 72 °C for 1 min. Construction of the 5′ H162G megaprimer required slightly different conditions to optimize product. Amplification was carried out by the PCR using pETpaDH as a template, the reverse mutagenic primer described above, a specific outside primer described previously (*20*), dNTPs, Triplemaster polymerase, and tuning buffer according to protocols for GC-rich templates (Eppendorf) by using a temperature program of 98 °C for 5 min, followed by 45 cycles of 98 °C for 20 s, 53 °C for 10 s, and 72 °C for 90 s. After Qiaquick purification, the 5′ and 3′ megaprimers, the specific outside end primers described previously, dNTPs, Triplemaster polymerase, and tuning buffer were combined for a PCR with a temperature program of 98 °C for 5 min, followed by 45 cycles of 98 °C for 20 s, 53 °C for 10 s, and 72 °C for 90 s. The resulting H162G *Pa* DDAH coding sequence was subsequently cloned between the *Nde*I and *Eco*RI restriction enzyme sites of a pET-28a expression vector as described previously (*20*). Expression and purification of mutant H162G *Pa* His_6-DDAH as well as C249S and wild-type *Pa* His_6-DDAH were completed as described previously (*20*).

Construction of an Expression Vector for PAD4. The human peptidylarginine deiminase-IV (PAD4) coding sequence and an additional 75 untranslated base pairs following the stop codon were amplified from cDNA in an IMAGE clone template (ATCC 8417075) using PCR and two specific end primers, 5′-CCGAATTCATGGCCCAGGGGACATTGA-3′ and 5′-CCGAATTCGCGGCCGCGAGCTCTTGCTTGCCACAC-3′, that were first described elsewhere (*26*). The forward primer contains an *Eco*RI restriction site (underlined) followed by 19 bases corresponding to the coding sequence of the PAD4 gene. The reverse primer contains a *Not*I restriction site (underlined) followed by 19 bases corresponding to the 3′-untranslated region. Amplification of the PAD4 coding sequence was carried out by PCR using an MJ Research PTC 200 thermocycler, along with the primers mentioned above, template DNA, dNTPs, and Triplemaster PCR reagents, following a temperature program: 95 °C for 5 min, followed by 30 cycles of 95 °C for 30 s, 52 °C for 30 s, and 72 °C for 1.5 min. The amplified sequence was purified using a Qiaquick kit, combined with pGEX-6P1 (Amersham Biosciences, Piscataway, NJ) in a 6:1 insert:vector ratio, and incubated at 37 °C for 4 h with *Not*I and *Eco*RI restriction enzymes. The resulting digestion products were purified using a Qiaquick kit and ligated together by incubation with T4 DNA ligase (Fisher, Pittsburgh, PA) for 10 h at 14 °C. The ligation mixture was concentrated by pellet paint precipitation (Novagen, San Diego, CA), and *Escherichia coli* DH5αE cells were transformed with the resulting plasmid (pGEX-hPAD4) for purification, sequencing, and storage.

Overexpression and Purification of PAD4. An overnight culture (10 mL) of codon-optimized *E. coli* Rosetta cells (Novagen, Madison, WI) harboring the pGEX-PAD4 expression plasmid was used to inoculate TB medium (1 L) containing ampicillin (50 μg/mL) and chloramphenicol (20 μg/mL) and was incubated in 4 L baffled flasks with shaking (300 rpm) at 37 °C until the cell density reached an OD_{600} of 1. The cultures were then cooled to 27 °C, and isopropyl β-D-thiogalactopyranoside (0.3 mM) was added to induce expression. After 15 h of continued expression at 27 °C, cells were harvested by centrifugation and the cell pellets frozen at −20 °C. Frozen cell pellets from 1 L of culture medium were resuspended in 300 mL of binding buffer [140 mM NaCl, 2.7 mM KCl, 10 mM Na_2HPO_4, and 1.8 mM KH_2PO_4 (pH 7.3)] containing 1 mL of a protease inhibitor cocktail for bacterial cells (Sigma-Aldrich Chemical Co.). Cell suspensions were sonicated on ice for 10 cycles of a 15 s pulse followed by a 120 s cooling interval. Cell debris was removed by centrifugation at 23500*g* for 30 min. The resulting supernatant was diluted with 200 mL of binding buffer, loaded onto a 10 mL glutathione−Sepharose-4 fast flow affinity resin column (Amersham Biosciences), and washed with 10 column volumes of binding buffer. The GST−PAD4 fusion protein was then eluted with reduced glutathione (10 mM) in Tris-HCl buffer (50 mM) and dithiothreitol (1 mM) at pH 8.0. Fractions containing active GST−hPAD4 fusion protein were pooled and dialyzed against three changes of 4 L of Tris-HCl (100 mM, pH 7.6) to remove excess glutathione, frozen in 0.25 mL aliquots (using liquid N_2), and stored at −80 °C. From 1 L of culture medium, this procedure yields 22 mg of purified GST−PAD4 fusion protein that is >90% homogeneous as assessed by SDS−PAGE stained with Pierce (Rockford, IL) GelCode Blue stain reagent.

Time-Dependent Inactivation of DDAH by 2-Chloroacetamidine (5). Purified recombinant His_6-tagged *Pa* DDAH (7.9 μM) was incubated with KCl (100 mM) and 2-chloroacetamidine (**5**, 0−10.5 mM) at pH 6.2 and 25 °C in MES buffer (10 mM) that was previously treated with Chelex-100 (Bio-Rad) to remove trace metal ions.

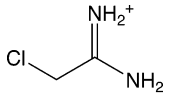

5

To test for time-dependent loss of activity, aliquots were removed from these incubations at time points (0−40 min) and diluted into an assay solution containing an excess (1 mM) of the alternative substrate, *S*-methyl-L-thiocitrulline (*20*). The remaining enzyme activity was assayed by detecting methanethiol release upon substrate hydrolysis using dithiobis(2-nitrobenzoic acid), as described elsewhere (*12*). Inactivation rates in preincubation mixtures, including enzyme, **5**, and an excess of the substrate N^{ω}-methyl-L-arginine (10 mM), were assessed to determine whether **5** acts at the active site of the enzyme. To avoid errors inherent in fitting linearized semilog plots, the observed pseudo-first-order inactivation rate constants (k_{obs}) were determined by direct fitting of the inactivation plots to a single-exponential equation. The resulting k_{obs} values were plotted against inactivator concentration and directly fit to the equation $k_{obs} = (k_{inact}[I])/(K_I + [I])$ to obtain K_I and k_{inact} values (*23*). All fits were calculated using KaleidaGraph (Synergy Software, Reading, PA). To further assay the irreversibility of inhibition by **5**, fully inhibited DDAH was dialyzed for 24 h at 4 °C with MES buffer (10 mM) and KCl (100 mM) at pH 6.2, and the resulting activity was assayed as described above. Control reactions were conducted in parallel to ensure that uninhibited DDAH retained activity under these conditions.

Time-Dependent Inactivation of PAD4 by 5. Incubations of purified recombinant GST−PAD4 fusion protein (2.4 μM), dithiothreitol (5 mM), $CaCl_2$ (10 mM), and **5** (0−30 mM) were tested for time-dependent loss of activity by removing aliquots (10 μL) from inactivation mixtures at each time point, and measuring the remaining enzyme activity by diluting into an assay solution (200 μL) containing an excess (5 mM) of substrate, N^{α}-benzoyl-L-arginine ethyl ester, and dithiothreitol (5 mM) in Tris-HCl buffer (100 mM) at pH 7.6 and 37 °C. Activity assays were incubated for 10 min each and then reactions quenched upon addition of 5 μL of trichloroacetic acid (6 M). Formation of product, N^{α}-benzoyl-L-citrulline ethyl ester, was assessed by derivatization and quantification of the resulting chromophore at 540 nm using a Cary 50 UV−vis spectrophotometer (Varian, Inc., Walnut Creek, CA) as described elsewhere (*12*, *27*, *28*). Assays were preformed at least in triplicate, and the resulting data were fit as described above.

Mass Spectral Analysis of Inactivated DDAH and DDAH Mutants. To characterize any covalent adducts formed during enzyme inactivation, 30 min incubations of **5** (1 mM) with *Pa* His_6-tagged DDAH were carried out at 25 °C under the same conditions used in the preincubations described above and quenched with 0.5 M trichloroacetic acid. Similar

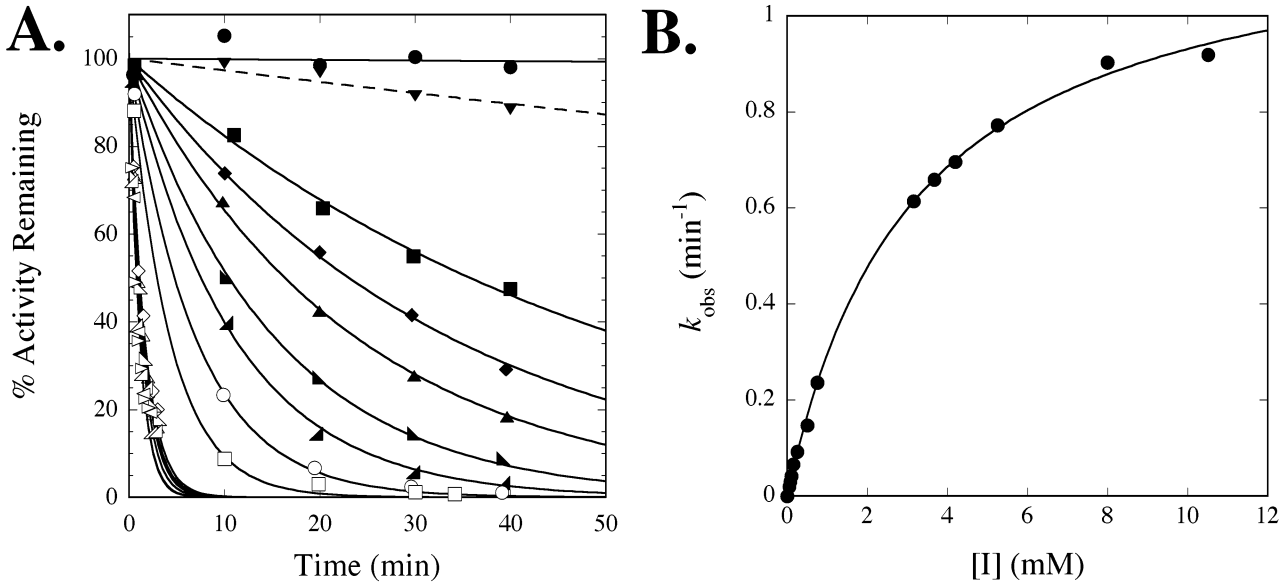

FIGURE 2: Time- and concentration-dependent inactivation of DDAH by **5**. (A) Exponential fits to the observed inactivation at pH 6.3 and 25 °C by different concentrations of **5**: 0 (●), 0.05 (■), 0.075 (◆), 0.1 (▲), 0.15 (filled right triangle pointing left), 0.25 (filled right triangle pointing right), 0.5 (○), 0.75 (□), 3.2 (◇), 3.7 (△), 4.2 (empty right triangle pointing left), 5.3 (empty right triangle pointing right), 8 (equilateral triangle pointing left), and 10.5 mM (equilateral triangle pointing right). The dashed line (▼) indicates fits to inactivation by **5** (0.1 mM) in the presence of 10 mM substrate, N^{ω}-methyl-L-arginine. (B) Concentration dependence of the pseudo-first-order k_{obs} values for inactivation.

incubations were carried out using the C249S and H162G mutant DDAH enzymes, and a wild-type DDAH that had previously been denatured in MES buffer (20 mM) containing 8 M urea at pH 6.2. Control reactions omitting **5** were also carried out in parallel. Samples were then desalted and analyzed by ESI-MS on a ThermoFinnigan LCQ (San Jose, CA) ion trap mass spectrometer as described previously (*20*).

Identification of a Covalently Modified DDAH Peptide. To determine the amino acid that is modified by **5**, the inactivated DDAH was exchanged into 50 mM ammonium acetate buffer (pH 4) by being passed through a Sephadex G-10 spin column, digested with Glu-C endoproteinase, and the products were analyzed using MALDI-TOF and MALDI-PSD on an Applied Biosystems Voyager-DE Pro as previously described (*20*, *29*). Theoretical digest masses were calculated by the MS-Digest program in the Protein Prospector suite using two missed cleavages (*30*).

Incubation of DDAH with 2-Chloroacetamide. Incubations containing DDAH (30 μM), KCl (100 mM), and 3 mM 2-chloroacetamide, a neutral analogue of **5**, were prepared at pH 6.2 and 25 °C in MES buffer (10 mM) that was previously treated with Chelex-100 to remove trace metal ions. To test for time-dependent loss of activity, aliquots were removed from these incubations at time points between 0 and 15 min and assayed as described above. Control reactions were completed in the absence of 2-chloroacetamide. All reactions were performed at least in triplicate, and the data were fit as described above.

RESULTS

Cloning, Expression, and Purification of Mutant and Wild-Type DDAH Enzymes. DNA sequencing of the H162G mutant indicated that the desired mutagenic codon was successfully incorporated, and no inadvertent mutations were introduced into the protein coding region. The resulting vector was used to express mutant H162G DDAH in BL21-(DE3) *E. coli*. This mutant, as well as the C249S and wild-type DDAH, was purified using published procedures (*20*) to greater than 95% homogeneity as assessed by SDS−PAGE and determined to contain less than 0.01 equiv of zinc by inductively coupled plasma mass spectrometry (Department of Geological Sciences, The University of Texas) (*20*).

Cloning, Expression, and Characterization of PAD4. DNA sequencing of pGEX-PAD4 indicated that there were no undesired mutations and that the coding sequence for PAD4 was correctly inserted in-frame after the sequence for an N-terminal glutathione transferase (GST) domain. From this expression plasmid, the resulting N-terminal GST-tagged protein was overexpressed in *E. coli* Rosetta cells (Novagen), and a single affinity chromatography step resulted in greater than 90% homogeneous wild-type GST−PAD4 fusion protein as assessed by SDS−PAGE (Supporting Information). The purified fusion protein hydrolyzes N^{α}-benzoyl-L-arginine ethyl ester with k_{cat} (1.6 ± 0.1 s^{-1}) and K_M (0.95 ± 0.09 mM) values at pH 7.6 and 37 °C similar to those reported previously for PAD4 without an N-terminal GST fusion (*27*), so the affinity tag was retained for the experiments reported here.

*Time-Dependent Inactivation of DDAH by **5** and by 2-Chloroacetamide.* Preincubation mixtures of DDAH with **5** result in time- and concentration-dependent enzyme inactivation, with K_I and k_{inact} values of 3.1 ± 0.8 mM and 1.2 ± 0.1 min^{-1}, respectively (Figure 2). Coincubation with excess substrate [uninhibited, $k_{cat} = 19$ min^{-1}, $K_M = 670$ μM (*20*)] protects against inactivation, indicating that **5** acts at the active site of the enzyme. Inhibition is observed after dilution of the preincubation mixtures into a large excess of substrate and after dialysis to remove noncovalently bound inhibitors, consistent with an irreversible mechanism. Pre-

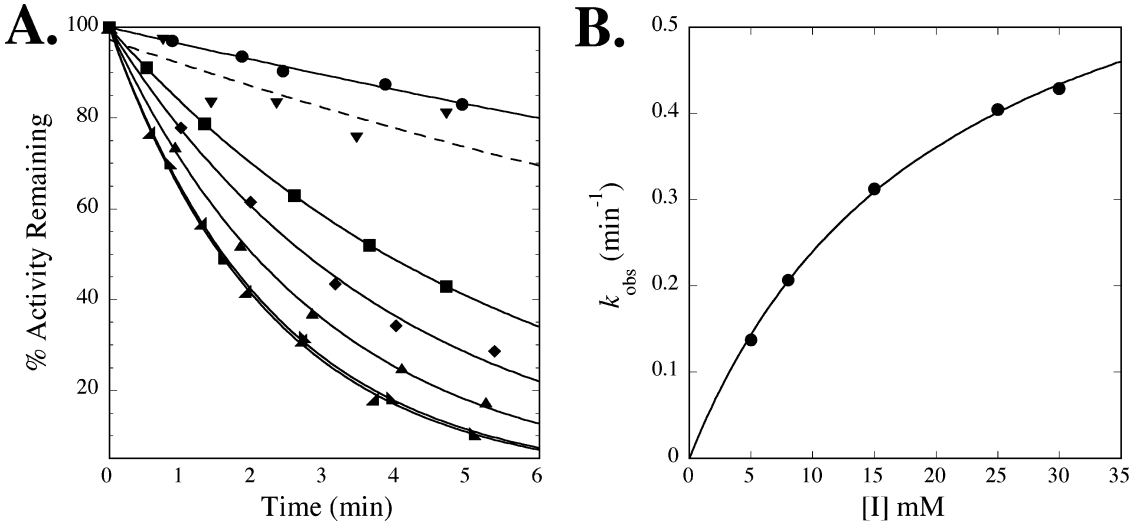

FIGURE 3: Time- and concentration-dependent inactivation of PAD4 by **5**. (A) Exponential fits to the observed inactivation of PAD4 at pH 7.6 and 37 °C with different concentrations of **5**: 0 (●), 5 (■), 8 (◆), 15 (▲), 25 (right triangle pointing left), and 30 mM (right triangle pointing right). The dashed line (▼) indicates fits to inactivation by **5** (15 mM) in the presence of 10 mM substrate, N^{α}-benzoyl-L-arginine ethyl ester. (B) Concentration dependence of the pseudo-first-order k_{obs} values for inactivation.

Table 1: Summary of Deconvoluted Protein Masses Observed in ESI-MS Spectra of Control and Inactivated DDAH

DDAH preparation	theoretical calc'd mass (Da)	control incubations with no inactivator, observed mass (Da)[a]	incubations with **5**, observed mass (Da)[a]
wild-type	30 503	30 499	30 556
urea-denatured	30 503	30 497	30 495
C249S	30 487	30 478	30 479
H162G	30 423	30 415	30 471

[a] The masses obtained from deconvoluted ESI-MS spectra are reported with errors of ±10 Da.

incubations with the neutral 2-chloroacetamide did not show any time-dependent inactivation relative to controls.

*Time-Dependent Inactivation of PAD4 by **5**.* Inactivation of PAD4 by **5** occurred with K_I and k_{inact} values of 20 ± 5 mM and 0.7 ± 0.1 min^{-1}, respectively (Figure 3). Addition of an excess of substrate (10 mM) to preincubation mixtures containing PAD4 and **5** (15 mM) drastically decreases the observed inactivation rate, indicating that substrate protects against inactivation and that **5** acts at the active site.

Mass Spectrum Analysis of Inactivated DDAH and DDAH Mutants. The deconvoluted mass spectrum of a control reaction mixture that included wild-type DDAH but no inactivator results in one major peak at 30 499 ± 10 Da, matching the mass calculated from the protein sequence, after removal of the N-terminal methionine residue (30 503 Da) (Table 1). Fully inactivated DDAH results in one major peak at a different mass of 30 556 ± 10 Da, indicating the addition of a covalent adduct of 57 ± 10 Da. Incubation mixtures with **5** and C249S DDAH, or urea-denatured DDAH, does not result in peaks that differ significantly from that predicted for the unmodified protein (Table 1). However, incubation mixtures with **5** and H162G DDAH do result in one major peak at 30 471 ± 10 Da, indicating a mass increase (56 ± 10 Da) over control incubations that do not contain inactivator (30 415 ± 10 Da).

Identification of a Covalently Modified DDAH Peptide. To determine which amino acid of DDAH is modified during inactivation, and to obtain a more precise mass of the covalent adduct, inactivated wild-type DDAH containing the +56 Da adduct was digested with Glu-C endoproteinase and the resulting peptides were detected using MALDI-TOF. Sixteen different peptides were identified by comparison with peptide molecular masses calculated from a theoretical digest. The observed peptides cover 66% of the total protein sequence and include active-site residues Cys249, His162, Glu114, and Thr165 (Table 2). The digestion mixture also shows a peptide at *m*/*z* 1789.1, which does not correspond to the mass of any predicted peptide after digestion, but is 56.1 ± 0.2 Da higher than that of the C-terminal peptide of DDAH ($_{240}$YRKIDGGVSCMSLRF$_{254}$) after digestion by Glu-C endoproteinase. This proposed adduct is consistent with the 57 ± 10 Da adduct found in undigested inactivated DDAH using ESI-MS. Similar mass increases were not

Table 2: Summary of Proteolytic Cleavage of Inactivated DDAH with Endoprotease Glu-C[a]

DDAH sequence positions plus leader (−18 to 0)	calc'd peptide mass (Da)	observed peptide mass (Da)[b]
−18 to 33	5657.4	5656.9
95−105	1324.5	1324.5
95−114	2277.6	2277.5
95−129	3914.5	3914.1
106−114	972.1	972.1
115−129	1655.9	1655.8
130−146	1832.1	1832.1
137−146	1102.3	1102.3
147−158	1282.5	1282.5
159−171	1485.8	1485.8
159−186	3093.6	3093.4
172−186	1626.8	1626.7
211−223	1546.8	1546.8
211−234	2846.4	2846.3
224−234	1318.6	1318.7
240−254	1733.1	1733.0
240−254 + Acam[c]	1789.2	1789.1

[a] Comparison of average calculated average peptide masses (MS-Digest in Protein Prospector) for up to two missed cleavages with experimental linear MALDI-TOF results. Amino acid numbering is assigned to match that of Protein Data Bank entry 1H70 (*11*). [b] The mass accuracy is 100 ppm, after smoothing of the spectrum and internal calibration. [c] Acam stands for the acetamidine adduct shown in Figure 4.

Table 3: Summary of Major Ions Observed in MALDI−PSD Fragmentation Spectra from *m*/*z* 1789 Parent Ion (YRKIDGGVSCMSLRF + Acam)[a]

ion	calcd *m*/*z*	observed *m*/*z*[b]
R	70	70
K	84	84
I/L	86	86
K	129	129
Y	136	136
RK-NH_3	268.3	268.1
b_2-NH_3	303.3	302.8
y_5	653.8	653.3
b_5	676.8	676.4
y_{10}	1057.3	−
y_{10}* + (Acam)[a]	1113.4	1113.9
y_{10}* − (Acam + S)	1023.2	1024.0
MH^+ − (Acam + S)	1699.0	1699.1

[a] Acam stands for the acetamidine fragment shown in Figure 4. [b] The mass accuracy is 1500 ppm. Average masses are reported.

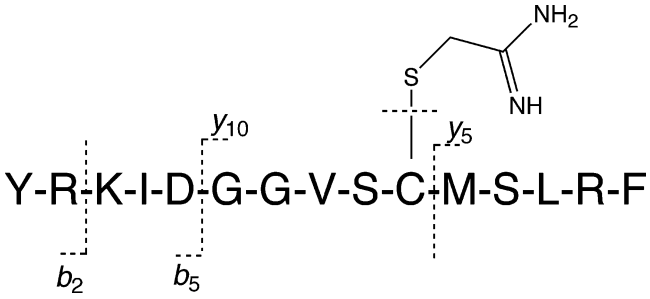

FIGURE 4: Summary of the fragmentation pattern from MALDI−PSD. A 1789 Da peptide shows b_2-NH_3, b_5, y_5, and y_{10}* fragments. The y_{10}* fragment ions have an additional mass shift of 56.6 Da due to the presence of the acetamidine adduct. Secondary fragmentation involving neutral loss of the acetamidine-modified cysteinyl sulfur implicates Cys249 as the point of attachment.

observed for any other peptides in the digest, including the peptide containing the active-site histidine residue (His162). A control Glu-C digest of DDAH lacking **5** did not contain any signal at *m*/*z* 1789, but did contain the unmodified C-terminal peptide at *m*/*z* 1733.

Ions from MALDI post-source decay (PSD) fragmentation spectra of the modified C-terminal peptide at *m*/*z* 1789 were used to provide information about the site of attachment (Table 3 and Figure 4). Ions found at *m*/*z* 84 and 129 are consistent with the singly charged multiple immonium and related ions characteristic of lysine and glutamine residues (*31*), but are both assigned here as lysine-derived ions (Table 3) because there are no glutamine residues found in the parent peptide. The b_2-NH_3, b_5, and y_5 daughter ions match those expected from unmodified peptide. However, a y_{10}* ion is found as a fragment containing the 56.6 ± 1.7 Da adduct. These results localize the adduct to a residue within the $_{245}$GGVSC$_{249}$ sequence. Additional fragmentation shows a neutral loss of 90 Da from the y^{10}* ion, providing additional information about the site of attachment (see below).

DISCUSSION

On the basis of the active-site similarities of DDAH and PAD (Figure 1), we proposed 2-chloroacetamidine (**5**) as a potential irreversible inhibitor of both enzymes. Preincubation mixtures of *Pa* DDAH with **5** result in time- and concentration-dependent enzyme inactivation, with K_I and k_{inact} values of 3.1 ± 0.8 mM and 1.2 ± 0.1 min^{-1}, respectively (Figure 2). Inhibition is observed after dilution of the preincubation mixtures into a large excess of substrate and after dialysis to remove any noncovalently bound inhibitors, consistent with an irreversible mechanism. Coincubation with excess substrate protects against inactivation, indicating that **5** acts at the active site of DDAH. Human PAD4 is also inactivated by **5** in a time- and concentration-dependent manner, can be protected from inactivation by excess substrate, cannot be reactivated upon dilution, and exhibits K_I and k_{inact} values of 20 ± 5 mM and 0.7 ± 0.1 min^{-1}, respectively (Figure 3), indicating that **5** is indeed capable of irreversibly inactivating two diverse members of the amidinotransferase superfamily. The higher K_I values observed with PAD4 may arise from the conformational flexibility of the active-site Cys and Asp residues that are known to change position upon binding calcium and substrate (*19*).

To determine how incubation with **5** leads to enzyme inactivation, the inhibition of DDAH was studied in more detail. Electrospray ionization (ESI) mass spectrometry was used to compare uninhibited and inactivated DDAH. The deconvoluted mass spectrum of a control reaction without **5** results in one major peak at 30 499 ± 10 Da, matching the mass calculated from the protein sequence, after removal of the N-terminal methionine residue (30 503 Da). Inactivated DDAH results in one major peak at a different mass of 30 556 ± 10 Da, indicating the addition of a covalent adduct of 57 ± 10 Da. This mass increase is consistent with the covalent addition of only 1 equiv of **5** with the loss of a Cl^- ion from **5**, and a proton from the enzyme (56.08 Da).

On the basis of the known active-site structure of DDAH (*11*) and the chemical similarity of **5** to chloromethyl ketone inhibitors, several reasonable inactivation mechanisms can be proposed. Active-site cysteine or histidine residues are most commonly targeted by chloromethyl ketones, although alkylation of other residues has been reported (*24*). Accordingly, the active-site His162 of DDAH may be covalently modified by one of the pathways depicted in Scheme 2. Alternatively, the active-site Cys249 may be covalently modified by one of the pathways shown in Scheme 3. Modification of the active-site His would be similar to the mechanism of chymotrypsin inactivation by (2*S*)-*N*-acetyl-L-alanyl-L-phenylalanyl α-chloroethane (*21*). Modification of the active-site Cys would be more similar to the mechanism of papain inactivation by chloromethyl ketones (*22*). To distinguish between these two possibilities, incubations of **5** with the H162G and C249S mutants of DDAH were analyzed for their ability to form a covalent adduct in the presence of either mutation. Both of these mutants are catalytically impaired and do not show significant turnover of the substrate N^{ω},N^{ω}-dimethyl-L-arginine (data not shown). The structure of the C249S mutant has previously been determined and shows only negligible differences from the wild-type structure (*11*). Incubation of the C249S mutant with **5** does not result in formation of a covalent adduct, suggesting that the nucleophilicity of this residue plays an important role in the inactivation mechanism (Table 1). However, incubation of **5** with the H162G mutant does result in formation of the +56 Da covalent adduct (Table 1). This result indicates that His162 is not required for modification by **5**, making histidine-dependent inactivation mechanisms (Scheme 2) unlikely.

Scheme 2: Possible Mechanisms for Modification of His162 by **5**

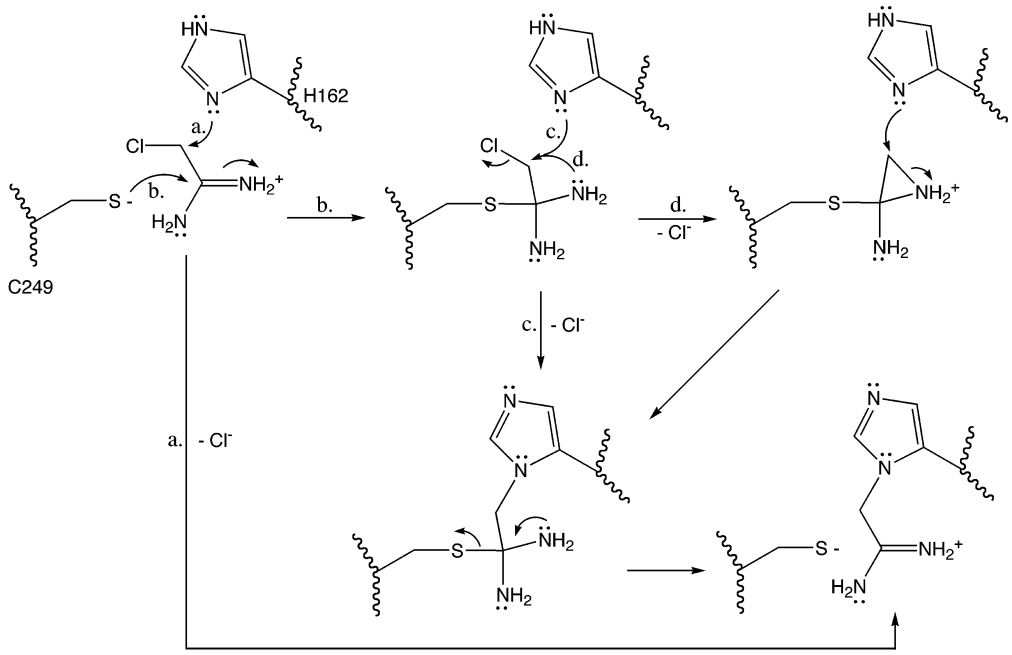

Scheme 3: Possible Mechanisms for Modification of Cys249 by (A) **5** or (B) 2-Chloroacetamide

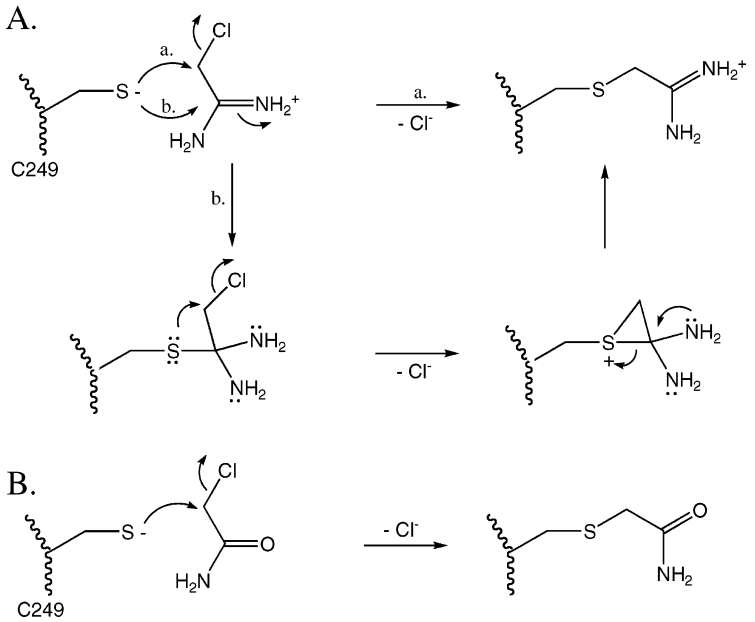

To test further the proposed inactivation mechanisms, we determined which residue of DDAH is modified by **5** by using protease digestion of control and inactivated wild-type enzyme and subsequent MALDI-TOF MS to identify the resulting peptide fragments. The linear MALDI spectrum of inactivated DDAH gives a new peak at 1789.1 ± 0.2 Da, corresponding to the mass of a C-terminal peptide containing the active-site cysteine ($_{240}$YRKIDGGVSCMSLRF$_{254}$) with an adduct of 56.1 ± 0.2 Da. Similar mass increases were not observed for any other peptides in the digest, including the peptide containing the active-site His162, and were not observed in control incubations lacking **5**. This result provides strong evidence that the single covalent modification observed above is attached to a residue within this peptide, most likely the active-site Cys249. The 100 ppm mass accuracy of the MALDI-MS measurements also allows us to distinguish between a covalent acetamidine adduct with a calculated mass difference of 56.08 Da (Scheme 3A), and a covalent acetamide adduct with a calculated mass addition of 57.06 Da (Scheme 3B) in the singly charged peptide ions. The acetamide adduct could potentially arise through hydrolysis of the amidine either before (Scheme 3B) or after (not shown) inactivation. Although only a small difference of 1 Da is predicted between these two adducts, accurate MS measurements can easily distinguish the 1 Da difference between arginine and citrulline residues arising from post-translational modifications (*32*). Here, the observed *m*/*z* increase of 56.1 ± 0.2 Da upon inactivation is consistent with formation of a covalently attached acetamidine adduct (Scheme 3A) and not consistent with an acetamide adduct (Scheme 3B). In support of this conclusion, no time-dependent inhibition was observed upon preincubation of

DDAH with the neutral 2-chloroacetamide under experimental conditions similar to those used for inactivation of DDAH by **5**.

Ions from MALDI post-source decay (PSD) fragmentation spectra of the modified C-terminal peptide at *m*/*z* 1789 provided additional information about the site of attachment (Table 3 and Figure 4). The b_2-NH_3, b_5, and y_5 ions match those expected from the unmodified peptide, but the y_{10}* ion represents a fragment containing a 56.6 ± 1.7 Da adduct, further localizing the point of attachment to $_{245}$GGVSC$_{249}$. Additional fragmentation shows a loss of 90 Da from the y^{10}* ion, representing the loss of the proposed covalent adduct when secondary fragmentation occurs between a Cβ−S bond, thereby implicating the sole cysteine residue in this peptide, Cys249 (the active-site cysteine), as the point of attachment (Figure 4). These results support the proposal that inactivation of DDAH occurs by either a direct attack of the active-site Cys249 on the methylene carbon of **5**, displacing a Cl^- ion and resulting in a stable thioether bond (Scheme 3A, a), or occurs through a sulfonium intermediate (Scheme 3A, b), analogous to mechanisms proposed for halomethyl ketone inactivation of some cysteine proteases (*33*).

The similarity of **5** to known DDAH substrates, its saturation inactivation kinetics, and the selective modification of the active-site Cys but not the four other Cys residues in *Pa* DDAH suggest that **5**, despite its small size, is bound specifically at the active site of the enzyme, albeit with modest affinity. In other studies (*34*−*37*), **5** has been used for the chemical rescue of proteins containing Arg (or Lys) that have been mutated to Cys, but previously (*34*, *35*), and in this report, **5** does not modify cysteine residues nonspecifically, but rather targets cysteine residues with a neighboring binding site for a guanidinium group, formed either by mutation, or, in the case of DDAH, by the natural substrate binding site. To illustrate this point, we found that control incubation mixtures containing **5** and urea-denatured DDAH do not result in adduct formation (Table 1). Also, the active-site Cys249 does not react indiscriminately with electrophiles such as the neutral 2-chloroacetamide or 5,5′-dithiobis(2-nitrobenzoic acid) (*12*) when incubated under similar reaction conditions. Active-site features which are conserved in the amidinotransferase superfamily (Figure 1) likely allow the inactivation of PAD4 by **5** despite the low level of overall amino acid identity (18%) between its catalytic domain and *Pa* DDAH.

The inactivation of these enzymes by **5** is similar to some chloromethyl ketone-mediated inactivation mechanisms. In general, the halomethyl ketones have proven to be extremely helpful in elucidating catalytic mechanisms of purified serine and cysteine proteases (*23*), in assaying distinct enzyme activities in proteomic extracts (*38*), and in probing biochemical pathways in living cells (*39*). One can envision that **5** and derivatives thereof may potentially serve a similar role for the amidinotransferase superfamily. Techniques such as SAR by NMR (*40*) and extended tethering (*41*) have proved the usefulness of low-affinity fragments in developing highly effective inhibitors. Hence, structural elaboration of **5** to increase affinity, selectivity, detectability, or bioavailability may allow a wide range of applications. For example, the DDAH isozymes are thought to be regulated by nitrosative stress (*5*, *42*, *43*), so the possibility of using derivatives of **5** to track changes in enzyme activity in complex mixtures is particularly attractive.

In summary, 2-chloroacetamidine is an active site-directed, time-dependent inactivator that targets the active-site cysteine residue of DDAH and likely inactivates PAD4 through a similar mechanism. These results suggest that **5** may serve as a general pharmacophore for inactivating this superfamily of enzymes and that incorporation of additional functional groups could allow a wide range of applications in activity-based protein profiling (*44*), investigation of biochemical pathways and catalytic mechanisms, and the design of future therapeutics.

ACKNOWLEDGMENT

We thank Laura McGonigal for assistance in preparing GST-hPAD4.

SUPPORTING INFORMATION AVAILABLE

One figure of an SDS−PAGE gel showing purified GST−PAD4 fusion protein. This material is available free of charge via the Internet at http://pubs.acs.org.

REFERENCES

1. Shirai, H., Blundell, T. L., and Mizuguchi, K. (2001) A novel superfamily of enzymes that catalyze the modification of guanidino groups, *Trends Biochem. Sci. 26*, 465−8.
2. Tocilj, A., Schrag, J. D., Li, Y., Schneider, B. L., Reitzer, L., Matte, A., and Cygler, M. (2005) Crystal structure of *N*-succinylarginine dihydrolase AstB, bound to substrate and product, an enzyme from the arginine catabolic pathway of *Escherichia coli*, *J. Biol. Chem. 280*, 15800−8.
3. Vallance, P., and Leiper, J. (2002) Blocking NO synthesis: How, where and why? *Nat. Rev. Drug Discovery 1*, 939−50.
4. Vossenaar, E. R., Zendman, A. J., van Venrooij, W. J., and Pruijn, G. J. (2003) PAD, a growing family of citrullinating enzymes: Genes, features and involvement in disease, *BioEssays 25*, 1106−18.
5. Knipp, M., Braun, O., and Vasak, M. (2005) Searching for DDAH inhibitors: *S*-Nitroso-L-homocysteine is a chemical lead, *J. Am. Chem. Soc. 127*, 2372−3.
6. Stuhlinger, M. C., Tsao, P. S., Her, J. H., Kimoto, M., Balint, R. F., and Cooke, J. P. (2001) Homocysteine impairs the nitric oxide synthase pathway: Role of asymmetric dimethylarginine, *Circulation 104*, 2569−75.
7. McGraw, W. T., Potempa, J., Farley, D., and Travis, J. (1999) Purification, characterization, and sequence analysis of a potential virulence factor from *Porphyromonas gingivalis*, peptidylarginine deiminase, *Infect. Immun. 67*, 3248−56.
8. Rossiter, S., Smith, C. L., Malaki, M., Nandi, M., Gill, H., Leiper, J. M., Vallance, P., and Selwood, D. L. (2005) Selective substrate-based inhibitors of mammalian dimethylarginine dimethylaminohydrolase, *J. Med. Chem. 48*, 4670−8.
9. Santa Maria, J., Vallance, P., Charles, I. G., and Leiper, J. M. (1999) Identification of microbial dimethylarginine dimethylaminohydrolase enzymes, *Mol. Microbiol. 33*, 1278−9.
10. Dowling, R. B., Newton, R., Robichaud, A., Cole, P. J., Barnes, P. J., and Wilson, R. (1998) Effect of inhibition of nitric oxide synthase on *Pseudomonas aeruginosa* infection of respiratory mucosa in vitro, *Am. J. Respir. Cell Mol. Biol. 19*, 950−8.
11. Murray-Rust, J., Leiper, J., McAlister, M., Phelan, J., Tilley, S., Santa Maria, J., Vallance, P., and McDonald, N. (2001) Structural insights into the hydrolysis of cellular nitric oxide synthase inhibitors by dimethylarginine dimethylaminohydrolase, *Nat. Struct. Biol. 8*, 679−83.
12. Stone, E. M., and Fast, W. (2005) A continuous spectrophotometric assay for dimethylarginine dimethylaminohydrolase activity, *Anal. Biochem. 343*, 335−7.
13. Knipp, M., Charnock, J. M., Garner, C. D., and Vasak, M. (2001) Structural and functional characterization of the Zn(II) site in dimethylargininase-1 (DDAH-1) from bovine brain. Zn(II) release activates DDAH-1, *J. Biol. Chem. 276*, 40449−56.

14. Suzuki, A., Yamada, R., Chang, X., Tokuhiro, S., Sawada, T., Suzuki, M., Nagasaki, M., Nakayama-Hamada, M., Kawaida, R., Ono, M., Ohtsuki, M., Furukawa, H., Yoshino, S., Yukioka, M., Tohma, S., Matsubara, T., Wakitani, S., Teshima, R., Nishioka, Y., Sekine, A., Iida, A., Takahashi, A., Tsunoda, T., Nakamura, Y., and Yamamoto, K. (2003) Functional haplotypes of PADI4, encoding citrullinating enzyme peptidylarginine deiminase 4, are associated with rheumatoid arthritis, *Nat. Genet. 34*, 395−402.
15. Denman, R. B. (2005) PAD: The smoking gun behind arginine methylation signaling? *BioEssays 27*, 242−6.
16. Lee, Y. H., Coonrod, S. A., Kraus, W. L., Jelinek, M. A., and Stallcup, M. R. (2005) Regulation of coactivator complex assembly and function by protein arginine methylation and demethylimination, *Proc. Natl. Acad. Sci. U.S.A. 102*, 3611−6.
17. Kearney, P. L., Bhatia, M., Jones, N. G., Yuan, L., Glascock, M. C., Catchings, K. L., Yamada, M., and Thompson, P. R. (2005) Kinetic characterization of protein arginine deiminase 4: A transcriptional corepressor implicated in the onset and progression of rheumatoid arthritis, *Biochemistry 44*, 10570−82.
18. Pritzker, L. B., and Moscarello, M. A. (1998) A novel microtubule independent effect of paclitaxel: The inhibition of peptidylarginine deiminase from bovine brain, *Biochim. Biophys. Acta 1388*, 154−60.
19. Arita, K., Hashimoto, H., Shimizu, T., Nakashima, K., Yamada, M., and Sato, M. (2004) Structural basis for Ca^{2+}-induced activation of human PAD4, *Nat. Struct. Mol. Biol. 11*, 777−83.
20. Stone, E. M., Person, M. D., Costello, N. J., and Fast, W. (2005) Characterization of a transient covalent adduct formed during dimethylarginine dimethylaminohydrolase catalysis, *Biochemistry 44*, 7069−78.
21. Kreutter, K., Steinmetz, A. C., Liang, T. C., Prorok, M., Abeles, R. H., and Ringe, D. (1994) Three-dimensional structure of chymotrypsin inactivated with (2*S*)-*N*-acetyl-L-alanyl-L-phenylalanyl α-chloroethane: Implications for the mechanism of inactivation of serine proteases by chloroketones, *Biochemistry 33*, 13792−800.
22. Drenth, J., Kalk, K. H., and Swen, H. M. (1976) Binding of chloromethyl ketone substrate analogues to crystalline papain, *Biochemistry 15*, 3731−8.
23. Plapp, B. V. (1982) Application of affinity labeling for studying structure and function of enzymes, *Methods Enzymol. 87*, 469−99.
24. Shaw, E. (1967) Site-specific reagents for chymotrypsin and trypsin, *Methods Enzymol. 11*, 677−86.
25. Ho, S. N., Hunt, H. D., Horton, R. M., Pullen, J. K., and Pease, L. R. (1989) Site-directed mutagenesis by overlap extension using the polymerase chain reaction, *Gene 77*, 51−9.
26. Nakashima, K., Hagiwara, T., Ishigami, A., Nagata, S., Asaga, H., Kuramoto, M., Senshu, T., and Yamada, M. (1999) Molecular characterization of peptidylarginine deiminase in HL-60 cells induced by retinoic acid and 1-α-2,5-dihydroxyvitamin D_3, *J. Biol. Chem. 274*, 27786−92.
27. Nakayama-Hamada, M., Suzuki, A., Kubota, K., Takazawa, T., Ohsaka, M., Kawaida, R., Ono, M., Kasuya, A., Furukawa, H., Yamada, R., and Yamamoto, K. (2005) Comparison of enzymatic properties between hPADI2 and hPADI4, *Biochem. Biophys. Res. Commun. 327*, 192−200.
28. Knipp, M., and Vasak, M. (2000) A colorimetric 96-well microtiter plate assay for the determination of enzymatically formed citrulline, *Anal. Biochem. 286*, 257−64.
29. Person, M. D., Monks, T. J., and Lau, S. S. (2003) An integrated approach to identifying chemically induced posttranslational modifications using comparative MALDI-MS and targeted HPLC-ESI-MS/MS, *Chem. Res. Toxicol. 16*, 598−608.
30. Clauser, K. R., Baker, P., and Burlingame, A. L. (1999) Role of accurate mass measurement (±10 ppm) in protein identification strategies employing MS or MS/MS and database searching, *Anal. Chem. 71*, 2871−82.
31. Falick, A. M., Hines, W. M., Medzihradszky, K. F., Baldwin, M. A., and Gibson, B. W. (1993) Low-mass ions produced from peptides by high-energy collision-induced dissociation in tandem mass spectrometry, *J. Am. Soc. Mass Spectrom. 4*, 882−93.
32. Kubota, K., Yoneyama-Takazawa, T., and Ichikawa, K. (2005) Determination of sites citrullinated by peptidylarginine deiminase using ^{18}O stable isotope labeling and mass spectrometry, *Rapid Commun. Mass Spectrom. 19*, 683−8.
33. Powers, J. C., Asgian, J. L., Ekici, O. D., and James, K. E. (2002) Irreversible inhibitors of serine, cysteine, and threonine proteases, *Chem. Rev. 102*, 4639−750.
34. Dhalla, A. M., Li, B., Alibhai, M. F., Yost, K. J., Hemmingsen, J. M., Atkins, W. M., Schineller, J., and Villafranca, J. J. (1994) Regeneration of catalytic activity of glutamine synthetase mutants by chemical activation: Exploration of the role of arginines 339 and 359 in activity, *Protein Sci. 3*, 476−81.
35. Wright, S. K., and Viola, R. E. (2001) Alteration of the specificity of malate dehydrogenase by chemical modulation of an active site arginine, *J. Biol. Chem. 276*, 31151−5.
36. Kravchuk, A. V., Zhao, L., Kubiak, R. J., Bruzik, K. S., and Tsai, M. D. (2001) Mechanism of phosphatidylinositol-specific phospholipase C: Origin of unusually high nonbridging thio effects, *Biochemistry 40*, 5433−9.
37. Messmore, J. M., Fuchs, D. N., and Raines, R. T. (1995) Ribonuclease A: Revealing Structure−Function Relationships with Semisynthesis, *J. Am. Chem. Soc. 117*, 8057−60.
38. Barglow, K. T., and Cravatt, B. F. (2004) Discovering disease-associated enzymes by proteome reactivity profiling, *Chem. Biol. 11*, 1523−31.
39. Amstad, P. A., Yu, G., Johnson, G. L., Lee, B. W., Dhawan, S., and Phelps, D. J. (2001) Detection of caspase activation in situ by fluorochrome-labeled caspase inhibitors, *BioTechniques 31*, 608−18.
40. Hajduk, P. J., Sheppard, G., Nettesheim, D. G., Olejniczak, E. T., Shuker, S. B., Meadows, R. P., Steinman, D. H., Carrera, J. G. M., Marcotte, P. A., Steverin, J., Walter, K., Smith, H., Gubbins, E., Simmer, R., Holzman, T. F., Morgan, D. W., Davidsen, S. K., Summers, J. B., and Fesik, S. W. (1997) Discovery of potent nonpeptide inhibitors of stromelysin using SAR by NMR, *J. Am. Chem. Soc. 119*, 5818−27.
41. Erlanson, D. A., Lam, J. W., Wiesmann, C., Luong, T. N., Simmons, R. L., DeLano, W. L., Choong, I. C., Burdett, M. T., Flanagan, W. M., Lee, D., Gordon, E. M., and O'Brien, T. (2003) In situ assembly of enzyme inhibitors using extended tethering, *Nat. Biotechnol. 21*, 308−14.
42. Leiper, J., Murray-Rust, J., McDonald, N., and Vallance, P. (2002) *S*-Nitrosylation of dimethylarginine dimethylaminohydrolase regulates enzyme activity: Further interactions between nitric oxide synthase and dimethylarginine dimethylaminohydrolase, *Proc. Natl. Acad. Sci. U.S.A. 99*, 13527−32.
43. Knipp, M., Braun, O., Gehrig, P. M., Sack, R., and Vasak, M. (2003) Zn(II)-free dimethylargininase-1 (DDAH-1) is inhibited upon specific Cys-*S*-nitrosylation, *J. Biol. Chem. 278*, 3410−6.
44. Jessani, N., and Cravatt, B. F. (2004) The development and application of methods for activity-based protein profiling, *Curr. Opin. Chem. Biol. 8*, 54−9.

BI051341Y